NJC

Accepted Manuscript

This article can be cited before page numbers have been issued, to do this please use: S. Lone, M. A. Bhat, R. Lone, S. Jameel, J. A. Lone and K. Bhat, *New J. Chem.*, 2018, DOI: 10.1039/C8NJ00063H.

ROYAL SOCIETY OF CHEMISTRY

rsc.li/njc

View Article Online
DOI: 10.1039/C8NJ00063H

Hemisynthesis, Computational and Molecular Docking studies of novel Nitrogen containing steroidal aromatase inhibitors: Testolactum and Testololactum

Shabir H. Lone[a,*], Muzzaffar A. Bhat[b], Rayees A. Lone[c,1], Salman Jameel[c,1], Javeed A. Lone[c], Khursheed A. Bhat*[, c]

[a]*Department of Chemistry, Govt Degree College Khanabal, Anantnag, Kashmir, India, 192101*

[b]*Department of Chemistry, Islamic University of Science and Technology, Awantipora, Kashmir, India, 192122.*

[c]*Bioorganic Chemistry Division Indian Institute of Integrative Medicine, Sanatnagar, Srinagar, Kashmir, India, 190005*

*Shabir Hussain Lone
Assistant Professor
Department of Chemistry
Govt Degree College Khanabal, Anantnag, Kashmir, India, 192101
Email: lone.shabir480@gmail.com

*Khursheed Ahmad Bhat
Senior Scientist
Bioorganic Chemistry Division
Indian Institute of Integrative Medicine, Sanatnagar, Srinagar, Kashmir, India, 190005
Email: kabhat@iiim.ac.in

[1]Both authors contributed equally

View Article Online
DOI: 10.1039/C8NJ00063H

Abstract

Testololactone (**10**) and Testolactone (**11**) represent the aromatase inhibitors containing lactone rings. We previously reported their hemisynthesis from the most common phytosterols which are highly abundant in nature. Herein, we report the synthesis of their nitrogen congeners: Testololactum (**3**) and Testolactum (**8**). The reaction process involves the conversion of 4-androstene-3,17-dione to its corresponding oxime using hydroxylamine hydrochloride whose beckmann rearrangement under acid conditions yielded the desired Testololactum (**3**). However Testolactum (**8**) was formed by the beckmann rearrangement of the oxime (**7**) of 1,4-androstene-3,17-dienone (**6**). This expeditious reaction scheme may be exploited for the bulk production of Testololactum (**3**) and Testolactum (**8**). Theoretical DFT studying structural and electronic properties of all the end products was carried out using the Becke three-parameter Lee-Yang-Parr function (B3LYP) and 6-31G (d,p) basis set. Molecular electrostatic potential map and frontier orbital analysis were carried out. HOMO-LUMO energy gap was calculated which allowed the calculation of relative reactivity descriptors like chemical hardness, chemical inertness, chemical potential, nucleophilicity and electrophilicity index of the synthesized products. Molecular docking studies of Testololactum (**3**), Testolactum (**8**) and Testololactone (**10**), with aromatase (CYP19) displayed binding free energies of (ΔG_b) = -9.85, -9.62 and -10.14 kcal/mol respectively compared to the standard Testolactone (**11**), a well-known aromatase inhibitor sold under the brand name TESLAC, which exhibited a binding free energy (ΔG_b) of -10.29 kcal/mol with inhibition constant K_i of 28.87 nM. The docking study revealed that nitrogen congeners exhibit relatively lower but appreciable therapeutic efficiency to be called as aromatase inhibitors.

Keywords: Testolactone; Testololactone; Testololactum; Testolactum; DFT; Docking

View Article Online
DOI: 10.1039/C8NJ00063H

Introduction

Around the globe, cancer is the leading cause of death with an estimated 7.6 million deaths during 2007 [1]. Apart from the cancers of skin, breast cancer is generally considered to be the most prevalent cancer in women and ranks second as a cause of tumor-related death only after lung cancer [2]. About two-thirds of breast related tumors require estrogens to grow and hence are called hormone-dependent [3]. Approximately 60% of pre-menopausal and 75% of post-menopausal cancers are hormone-dependant [4], implying that the endogenous estrogens are essentially required for proliferation. Therefore the drugs used against treatment of estrogen positive breast cancer involve obstruction of hormone production or hormone action. Cytochrome P450 19 (CYP19) commonly known as aromatase or estrogen synthase, has always been found to be the promising target for the treatment of breast cancer [5] because inhibition of aromatase enzyme leads to decreased estrogen production, thereby stopping/reducing the tumor-growth. To block estrogen production, compounds used are known as aromatase inhibitors (AIs). They represent the front line therapy for hormone dependent breast cancer [1] and are classified as steroidal and non-steroidal aromatase inhibitors. Among the steroidal aromatase inhibitors which exhibit this enzyme inhibition at nano-molar concentrations include Formestane, Exemestane, Testololactone and Testolactone (**Fig 1**) etc. Formestane a steroidal analogue was the first AI used in clinical trials and has been demonstrated to be effective as well as well tolerated [3,6]. Testolactone (**11**), marketed under the trade name TESLAC is regarded as a pioneer drug to treat breast cancer [7]. Similarly Exemestane sold under the brand name AROMASIN® is an irreversible aromatase inhibitor [8].

View Article Online
DOI: 10.1039/C8NJ00063H

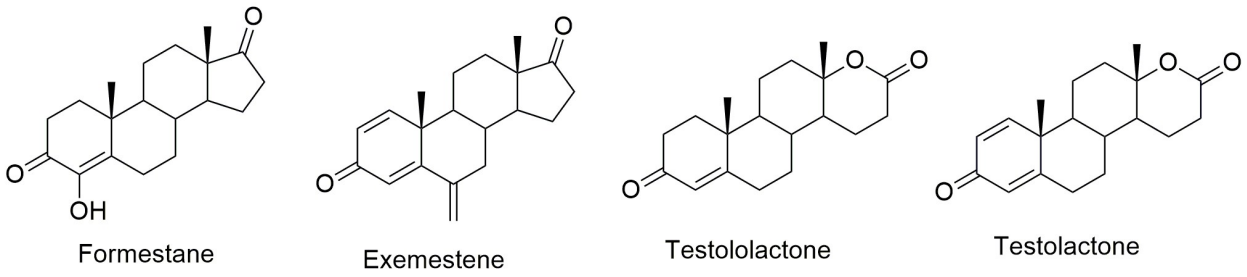

Fig 1. Some well-known steroidal aromatase inhibitors

So far there are a few literature reports which highlight the synthetic routes for the preparation of these aromatase inhibitors. [9-15]. Previously, we reported synthesis of Testololactone (**10**) and Testolactone (**11**) (**Fig 2**) using the naturally known abundant phytosterols like *β*-sitosterol and stigmasterol as precursors. Over the past decades few synthetic aromatase inhibitors have been reported but their theoretical investigations of structural, molecular and electronic properties using DFT or related computational methods still lack in the literature. However, in recent past a number of docking studies have been carried out to examine the exact mechanistic and binding mechanism of aromatase inhibitors [16-21]. Based on the aforementioned facts as well as our ongoing research program to search for natural product based medicinal leads [15, 22-33], particularly the development of new aromatase inhibitors, we turned our attention towards the hemisynthesis of nitrogen congeners of the well-known aromatase inhibitors and studied their electronic, structural and molecular properties along with their interaction mechanism with aromatase enzyme using computational and molecular docking studies for the first time across any part of the globe.

Results and discussion

4-androstene-3,17-dione (**1**) and 1,4-androstadien-3,17-dione (**6**) were synthesized from natural precursors like *β*-sitosterol, stigmasterol as described previously [15]. 4-Androstene-3,17-dione

View Article Online
DOI: 10.1039/C8NJ00063H

was then subjected to oxime formation at its 17-keto moiety using hydroxylamine hydrochloride to afford compound **2**. Formation of **2** was easily confirmed by the close analysis of its ^{13}C-NMR. Disappearance of carbon resonance at 222 ppm (due to 17-keto moiety in **1**) and the appearance of carbon signal at 175.33 ppm in **2** indicated its formation. Acid-catalyzed beckmann rearrangement of **2** resulted in an isomeric mixture of **3** and **4** in 4:1 ratio. Compound **3** which represents a nitrogen congener of Testololactone (**10**) (**Fig 2)** was hence forth named as Testololactum. The two isomers **3** and **4** were differentiated on the basis of their ^{13}C-NMR spectral data. Carbon signals at 54.34 (due to quarternary carbon-13) and 38.77 (due to CH_2 at position 16) of compound **3** indicated the N---C13 and CH_2 (position 16)------C=O linkages respectively. However in compound **4** carbon resonances at 44.89 and 48.21 ppm indicated C13-----C=O and N-------CH_2 (position 16) linkages respectively. To target the synthesis of better congener (**8**) as shown in **Fig 2** compound **1** was subjected to phenylselenation at position 2 of ring A using phenylselenyl chloride in ethyl acetate to afford the desired α-phenylselenide (**5**) whose degradation with hydrogen peroxide in dichloromethane afforded 1,4-androstadiene-3,17-dione (**6**)**.** Compound **6** was then subjected to oxime formation at its 17-keto moiety using hydroxylamine hydrochloride to afford **7** whose acid-mediated beckmann rearrangement yielded a mixture of compounds **8** and **9** in 4:1 ratio. Both **8** and **9** were characterized on the same grounds as that of **3** and **4**. Since **8** represents a nitrogen congener of Testolactone (**11),** it was therefore named as Testolactum (**8**). After having synthesized the target compounds, we next focussed on optimization of their structures using theoretical DFT. Optimization of structures is needed for carrying out molecular docking study. The theoretical study allowed the calculation of MEPS, FMO's, HUMO-LUMO energy gap and related reactivity descriptors which depicted the potential kinetic stability and reactivity of the target compounds.

View Article Online
DOI: 10.1039/C8NJ00063H

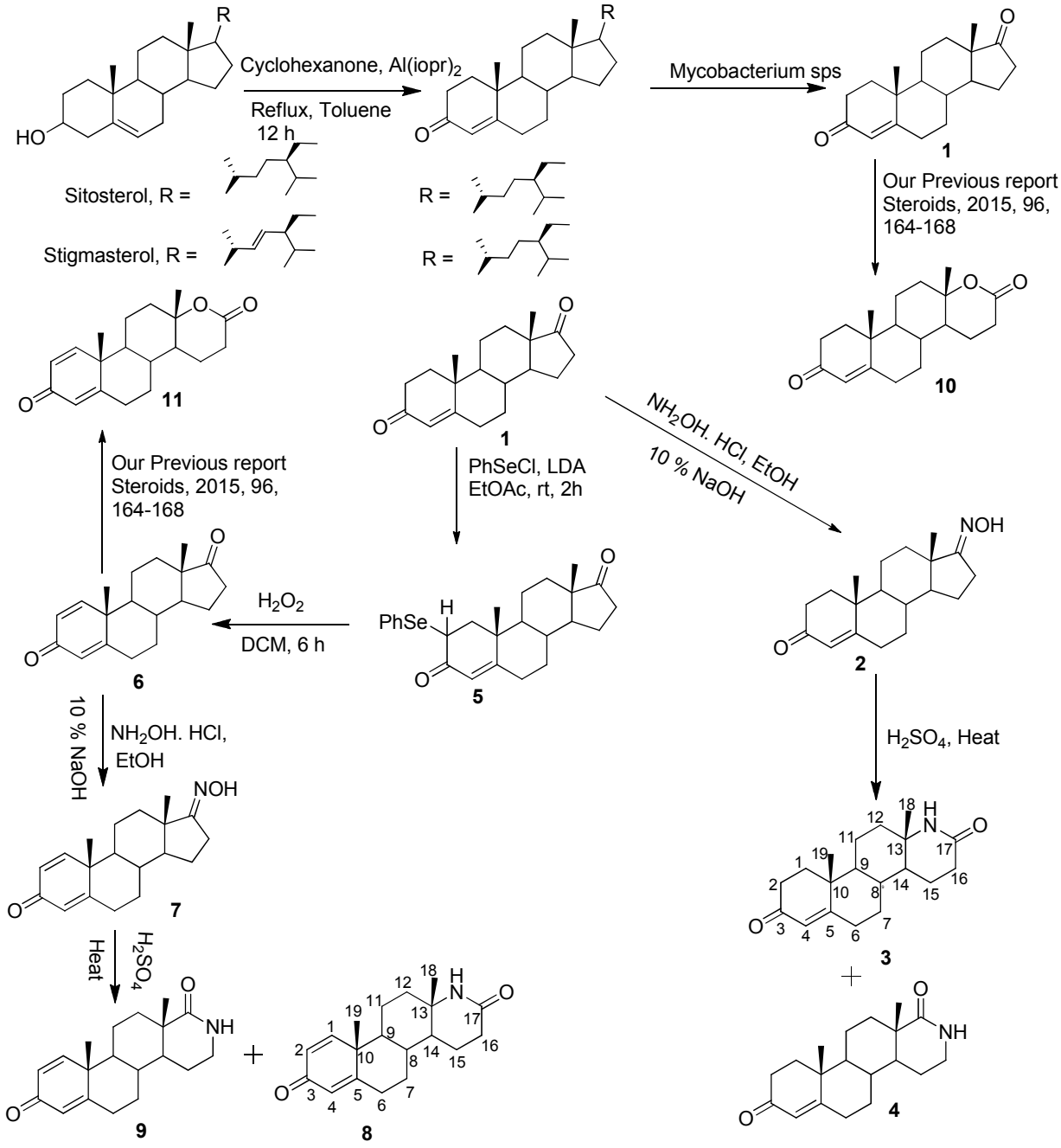

Fig 2. Synthesis of Testololactum (**3**) and Testolactum (**8**)

View Article Online
DOI: 10.1039/C8NJ00063H

MEP analysis

MEP is useful for predicting molecular reaction behavior. It is used to assess the molecular reactivity towards charged reactants and depict the hydrogen bond interactions. Molecular electrostatic surfaces reveal essential characteristics like size, shape and variation of electron density while correlating it with dipole moment, partial charges, electronegativity, and chemical reactivity sites located in the molecule. ESP is studied by computation organic chemists for analyzing drug-receptor and enzyme-substrate interactions along with H-bonding interactions [34-38]. **Fig 3** shows the MEP of compound **3, 8, 10** and **11**, calculated using B3LYP/6-31G (d,p) basis set. A comparative view of molecular electrostatic maps is presented here which are

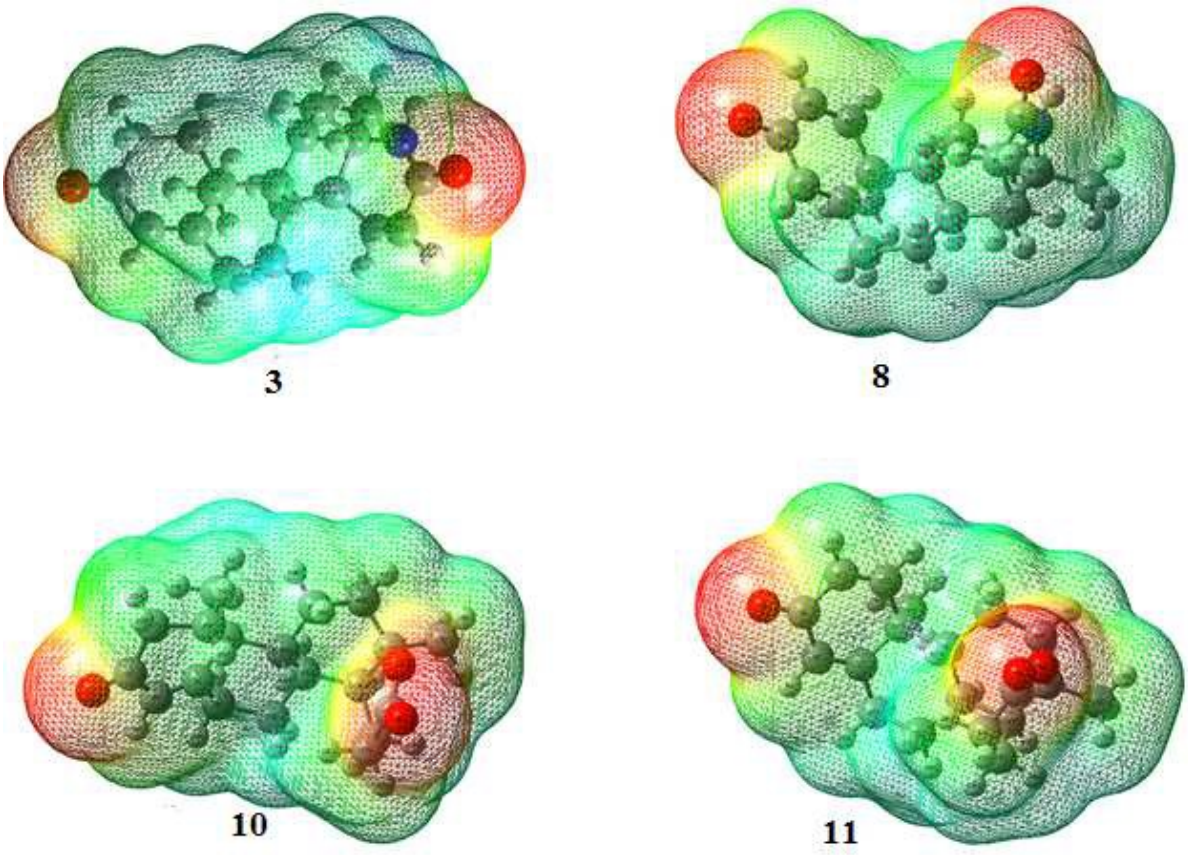

Fig 3. MEP of compounds **3**, **8**, **10** and **11** calculated using BL3YP/6-31G (d, p) basis set

View Article Online
DOI: 10.1039/C8NJ00063H

more or less similar. The pictorial representation with rainbow colour scheme of electrostatic potential lies in the range of -6.138e-2 to 6.138e-2, -6.315e-2 to +6.315e-2, -6.018e-2 to +6.108e-2 and -6.082e-2 to 6.082e-2 for compounds **3**, **8, 10** and **11** respectively. The darkest red regions indicate regions with high electron density (negative potential) while as the darkest blue regions indicate regions with low electron density (positive potential). As can be seen in the MEP for all the four compounds the regions around carbonyl oxygens at positions 3 and 17 of the steroidal skeletons are red and hence possess high electron density or in other words a site more vulnerable to electrophilic attack. This is quite consistent with the basic organic chemistry because carbonyl oxygen is electron rich and carbonyl carbon is electron deficient.

Frontier Molecular analysis

Frontier molecular orbitals (FMO) (**Fig 4**) help us to determine the electric and optical properties electronic transitions and kinetic stability [39]. FMO's of all four target compounds (**3**, **8**, **10** and **11**) were calculated using using BL3YP/6-31G (d, p) level of theory. As can be seen from **Fig. 4,** HOMO and LUMO are located over ring A of all the four steroid skeletons. The HOMO-LUMO energy gaps are 0.18571, 0.17798, 0.18527 and 0.17791 e. v for compounds **3**, **8**, **10** and **11** respectively. **(Table 1**). The small difference among the HOMO-LUMO energies of all the compounds depicts their similar nature of reactivity. This HOMO-LUMO energy gap was explored to evaluate the important chemical reactivity descriptors like softness, hardness, electronegativity, chemical potential, electron-affinity and ionization energy. Chemical hardness (η) and softness is basically the measurement of chemical reactivity to which the addition of charge stabilizes the system [40, 41] and chemical potential μ gives an idea about the transfer of charge from higher

View Article Online
DOI: 10.1039/C8NJ00063H

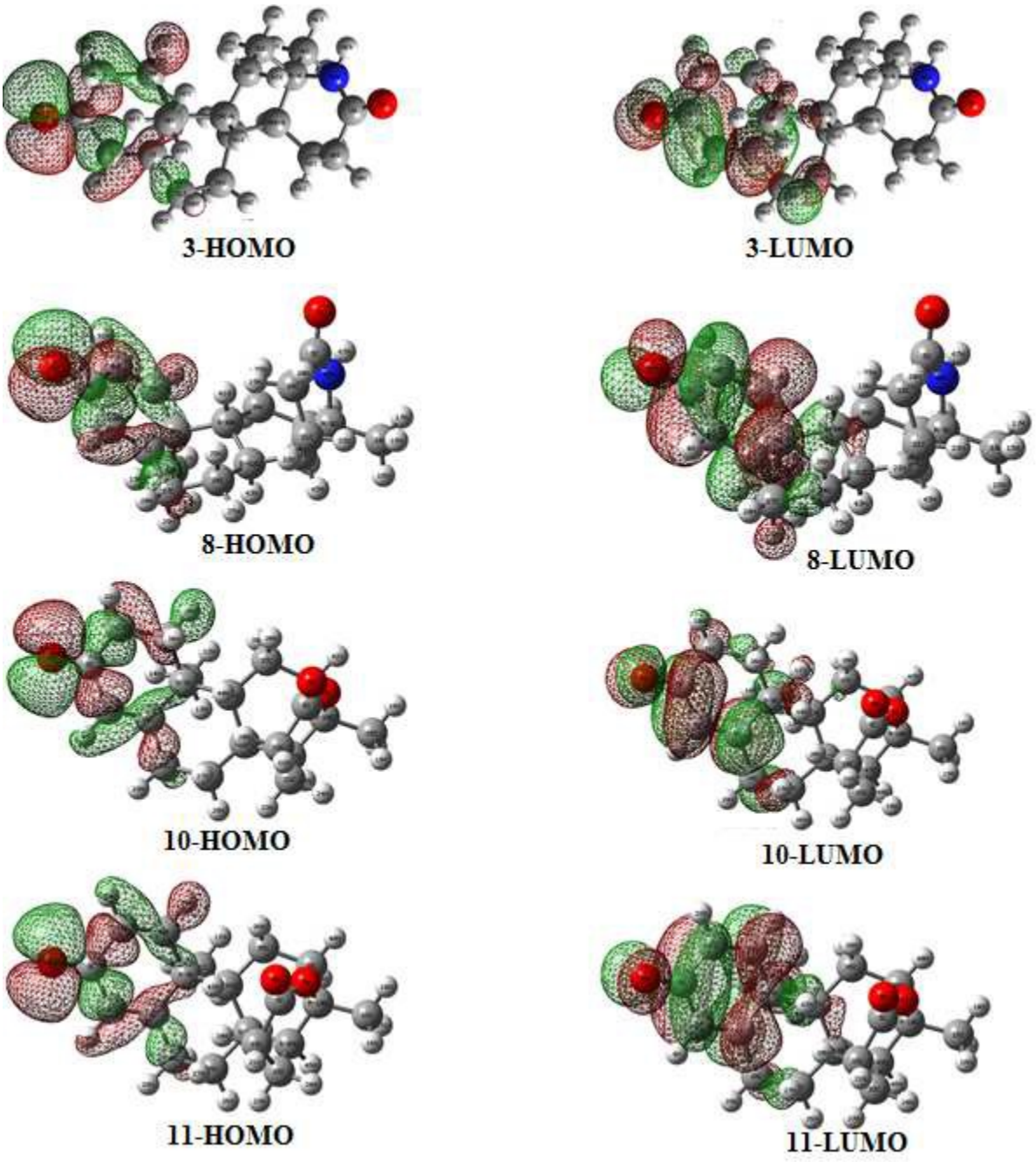

Fig 4 HOMO-LUMO surfaces of compound**s 3, 8, 10** and **11** simulated using BL3YP /6-31 G (d, p) level of theory.

potential to lower potential. Another important descriptor electronegativity (χ) represents the tendency to attract electrons. These properties have been defined as follows [42-44]:

View Article Online
DOI: 10.1039/C8NJ00063H

$$\eta = \frac{(I-A)}{2}, \quad \mu = \frac{-(I+A)}{2}, \chi = \frac{(I+A)}{2}$$

where I and A represent ionization potential and electron affinity of the compound, which are actually obtained from HOMO and LUMO energies as I = $-E_{HOMO}$ and A = $-E_{LUMO}$ as per Janak theorem [45] and Perdew et al. [46]. Using above equations these descriptors were calculated. Hardness (η) which is directly related to stability was found to be 0.09285, 0.08899, 0.09263 and 0.08895 e.v. for **3**, **8**, **10** and **11** respectively. Chemical potential 'μ' which is actually the escaping ability of electrons from an equilibrium system was found to be -0.140875, -0.14378, -0.140695 and -0.145295 for **3**, **8**, **10** and **11** respectively. The global electrophilicity index (ω), a global reactivity index that is related to chemical hardness and chemical potential and first introduced by Parr et al [44] represents the measure of the stabilization in energy achieved when the system acquires an additional electronic charge from the environment and is given by **ω** = $\mu^2/2\eta$. The corresponding values for compounds **3, 8, 10** and **11** are 0.10686, 0.11615, 0.10684 and 0.11865 e.v respectively. All these parameters have been calculated for the target compounds using B3LYP/6-31G (d, p) basis set and are depicted in **Table 1.**

Table 1: Calculated energy values for compounds **3, 8**, **10** and **11** using B3LYP/6-31G (d, p) basis set

Parameter	Compound 3	Compound 8	Compound 10	Compound 11
Energy (au)	-945.53034	-944.31317	-965.39716	-964.17202
Dipole moment (Debye)	1.4785	7.8287	6.7148	7.6207
E_{HOMO} (eV)	-0.23373	-0.23277	-0.23333	-0.23425
E_{LUMO} (eV)	-0.04802	-0.05479	-0.04806	-0.05634
$E_{HOMO-LUMO}$ (eV)	0.18571	0.17798	0.18527	0.17791
E_{HOMO-1} (eV)	-0.23760	-0.23889	-0.25770	-0.25846

View Article Online
DOI: 10.1039/C8NJ00063H

E_{LUMO+1} (eV)	0.03033	-0.00192	0.14433	0.01289
$E_{(HOMO-1)-(LUMO+1)}$ (eV)	0.26793	0.23697	0.40203	0.27135
Hardness (η)	0.09285	0.08899	0.09263	0.08895
Chemical Potential (μ)	-0.140875	-0.14378	-0.140695	-0.145295
Electronegativity (χ)	0.140875	0.14378	0.140695	0.145295
Electrophilicity index (ω)	0.10686	0.11615	0.10684	0.11865

From **Table 1,** it is clear that corresponding HOMO-LUMO energy gap and reactivity descriptors like hardness, potential and global electrophilicity of all the four compounds are more or less similar to each other, implying their nearly similar behaviour in enzyme-protien interaction study.

PASS and Molecular Docking

After having successfully optimized and calculated various reactivity descriptors for all the four compounds using DFT employing the well-known B3LYP/6-31G (d,p) basis function, we next studied their behaviour towards CYP19 enzyme. Before carrying out the actual analysis, it was envisaged to predict the pharmacological properties of these four compounds, particularly their performance towards CYP19 enzyme, using an available online PASS [47]. PASS is an important tool that evaluates the biological activity of a molecule in relation to its structure. It assesses the druglikeness and toxicities of molecules like teratogenicity, carcinogenicity embroyogenecity etc. The average accuracy of prediction is about 95 % according to leave-one-out-cross validation (LOOCV) estimation and the probabilities, Pa (Probable activity) and Pi (Probable inactivity), are values that vary from 0.000 to 1.000, and generally Pa + Pi $\neq$ 1 as these probabilities are calculated independently [48]. PASS analysis results of the desired compounds

View Article Online
DOI: 10.1039/C8NJ00063H

3, **8**, **10** and **11** have been enlisted in **Table 2** below. A thorough analysis of PASS result shows that the target compounds **3, 8, 10** and **11** are highly active as expected by the authors against

Table 2. PASS (Prediction Activity Spectra) of compounds **3**, **8**, **10** and **11** with Pa >0. 4.

Testololactum (3)					
Pa	**Pi**	**Activity**	**Pa**	**Pi**	**Activity**
0.971	0.002	Testosterone 17beta-dehydrogenase (NADP+) inhibitor	0.587	0.013	Anesthetic general
0.964	0.003	CYP2C12 substrate	0.616	0.042	Antineoplastic
0.925	0.003	CYP2J substrate	0.578	0.015	CYP3A3 substrate
0.918	0.003	CYP2J2 substrate	0.602	0.040	CYP3A4 substrate
0.911	0.003	Lysase inhibitor	0.564	0.004	Morphine 6-dehydrogenase inhibitor
0.881	0.003	CYP2B5 substrate	0.583	0.027	CYP3A5 substrate
0.844	0.003	Ovulation inhibitor	0.560	0.007	Indanol dehydrogenase inhibitor
0.840	0.003	CYP2A11 substrate	0.552	0.004	CYP2C8 inducer
0.836	0.004	27-Hydroxycholesterol 7alpha-monooxygenase inhibitor	0.557	0.009	Menopausal disorders treatment
0.820	0.003	CYP2A2 substrate	0.550	0.003	Testosterone agonist
0.798	0.002	CYP17 inhibitor	0.554	0.010	Interleukin 2 agonist
0.794	0.003	CYP2A1 substrate	0.620	0.077	Membrane permeability inhibitor
0.797	0.007	Oxidoreductase inhibitor	0.566	0.028	Alopecia treatment
0.790	0.003	CYP2A4 substrate	0.573	0.044	CYP3A substrate
0.787	0.004	CYP2C11 substrate	0.532	0.007	RELA expression inhibitor
0.768	0.003	Androgen antagonist	0.527	0.003	Estradiol 17alpha-dehydrogenase inhibitor
0.747	0.007	CYP3A1 substrate	0.536	0.012	CYP2C18 substrate
0.738	0.004	Acetylcholine neuromuscular blocking agent	0.546	0.024	Antipruritic, allergic
0.737	0.010	CYP3A4 inducer	0.524	0.004	Lipocortins synthesis antagonist
0.718	0.011	CYP3A inducer	0.528	0.008	CYP3A7 substrate
0.706	0.004	CYP2C9 inducer	0.518	0.003	CYP2A10 substrate
0.711	0.010	CYP3A2 substrate	0.539	0.026	Erythropoiesis stimulant
0.704	0.006	Prostate disorders treatment	0.523	0.012	DELTA14-sterol reductase inhibitor
0.695	0.004	Prostate cancer	0.539	0.030	Respiratory analeptic

View Article Online
DOI: 10.1039/C8NJ00063H

		treatment			
0.696	0.016	Prostaglandin-E2 9-reductase inhibitor	0.511	0.004	Steroid synthesis inhibitor
0.651	0.004	CYP2C6 substrate	0.509	0.003	Cholestenone 5alpha-reductase inhibitor
0.656	0.011	Dermatologic	0.507	0.004	CYP19 inhibitor
0.647	0.003	CYP7 inhibitor	0.534	0.033	CYP2C9 substrate
0.645	0.003	CYP2B11 substrate	0.515	0.014	Gonadotropin antagonist
0.634	0.004	CYP2G1 substrate	0.519	0.023	Steroid N-acetylglucosaminyltransferase inhibitor
0.631	0.004	CYP2A5 substrate	0.502	0.006	Antiacne
0.603	0.009	UGT1A4 substrate	0.558	0.062	Antiseborrheic
0.597	0.009	Gestagen antagonist	0.517	0.026	CYP2C19 substrate
0.606	0.027	CYP2C substrate	0.491	0.005	Cholesterol oxidase inhibitor
0.579	0.005	Prostatic (benign) hyperplasia treatment	0.524	0.047	JAK2 expression inhibitor

Testolactum (8)

Pa	Pi	Activity	Pa	Pi	Activity
0.926	0.004	Testosterone 17beta-dehydrogenase (NADP+) inhibitor	0.600	0.041	CYP3A4 substrate
0.919	0.008	CYP2C12 substrate	0.586	0.029	CYP2C substrate
0.822	0.016	CYP2J substrate	0.571	0.017	Antipruritic, allergic
0.801	0.004	CYP2B5 substrate	0.560	0.006	CYP7 inhibitor
0.796	0.014	CYP2J2 substrate	0.558	0.005	Prostatic (benign) hyperplasia treatment
0.788	0.011	Lysase inhibitor	0.587	0.041	Oxidoreductase inhibitor
0.738	0.003	CYP2C9 inducer	0.550	0.007	Indanol dehydrogenase inhibitor
0.719	0.011	CYP3A4 inducer	0.571	0.044	CYP3A substrate
0.710	0.007	CYP2C11 substrate	0.528	0.003	Lipocortins synthesis antagonist
0.703	0.012	CYP3A inducer	0.526	0.005	CYP2C8 inducer
0.696	0.006	Prostate disorders treatment	0.514	0.007	CYP2B11 substrate
0.691	0.007	CYP2A2 substrate	0.521	0.014	Muscular dystrophy treatment
0.686	0.004	CYP17 inhibitor	0.541	0.036	Alopecia treatment
0.686	0.005	Acetylcholine neuromuscular blocking agent	0.519	0.015	Gestagen antagonist
0.686	0.007	Ovulation inhibitor	0.529	0.029	Antipruritic
0.691	0.017	Antiinflammatory	0.512	0.015	Gonadotropin antagonist
0.680	0.015	27-Hydroxycholesterol 7alpha-monooxygenase	0.487	0.004	CYP19 inhibitor

View Article Online
DOI: 10.1039/C8NJ00063H

		inhibitor			
0.652	0.011	Dermatologic	0.479	0.005	Growth stimulant
0.645	0.005	Prostate cancer treatment	0.477	0.007	CYP2C6 substrate
0.635	0.004	Androgen antagonist	0.484	0.015	CYP2G1 substrate
0.629	0.009	CYP2A11 substrate	0.474	0.005	Thyroxine 5-deiodinase inhibitor
0.625	0.010	CYP2A1 substrate	0.504	0.039	CYP2C9 substrate
0.618	0.012	CYP2A4 substrate	0.496	0.031	Mannan endo-1,4-beta-mannosidase inhibitor
0.639	0.037	Antineoplastic	0.528	0.067	Antiseborrheic
0.604	0.028	CYP3A2 substrate	0.509	0.051	JAK2 expression inhibitor
0.589	0.022	CYP3A1 substrate	0.477	0.021	Menopausal disorders treatment
Testololactone (10)					
Pa	**Pi**	**Activity**	**Pa**	**Pi**	**Activity**
0.970	0.001	CYP19 inhibitor	0.723	0.006	CYP2C11 substrate
0.961	0.002	Testosterone 17beta-dehydrogenase (NADP+) inhibitor	0.708	0.002	CYP2B11 substrate
0.956	0.004	CYP2C12 substrate	0.689	0.003	CYP2G1 substrate
0.948	0.001	CYP2B5 substrate	0.684	0.009	Dermatologic
0.929	0.003	CYP2J substrate	0.682	0.010	Cholesterol antagonist
0.922	0.003	CYP2J2 substrate	0.674	0.006	Acetylcholine neuromuscular blocking agent
0.907	0.001	CYP2A4 substrate	0.670	0.014	CYP3A4 inducer
0.907	0.003	CYP3A1 substrate	0.667	0.012	HMOX1 expression enhancer
0.882	0.002	CYP2A11 substrate	0.661	0.009	Prostate disorders treatment
0.880	0.002	CYP2A1 substrate	0.656	0.004	Androgen antagonist
0.878	0.002	CYP2A2 substrate	0.665	0.014	CYP3A inducer
0.878	0.004	Lysase inhibitor	0.645	0.002	3-Oxosteroid 1-dehydrogenase inhibitor
0.869	0.005	Antineoplastic	0.640	0.002	Estradiol 17alpha-dehydrogenase inhibitor
0.824	0.004	CYP3A2 substrate	0.642	0.005	Gestagen antagonist
0.823	0.008	Prostaglandin-E2 9-reductase inhibitor	0.638	0.005	Menopausal disorders treatment
0.818	0.005	Oxidoreductase inhibitor	0.647	0.024	JAK2 expression inhibitor
0.792	0.006	27-Hydroxycholesterol 7alpha-monooxygenase inhibitor	0.623	0.011	CYP3A3 substrate
0.798	0.015	CYP3A4 substrate	0.618	0.005	Trans-1,2-dihydrobenzene-1,2-diol dehydrogenase inhibitor
0.784	0.004	Ovulation inhibitor	0.616	0.005	Prostate cancer treatment

View Article Online
DOI: 10.1039/C8NJ00063H

0.781	0.002	Aromatase inhibitor	0.613	0.004	CYP2A3 substrate
0.793	0.015	CYP3A substrate	0.622	0.013	Antiprotozoal (Leishmania)
0.779	0.008	CYP3A5 substrate	0.613	0.009	UGT2B substrate
0.764	0.003	CYP17 inhibitor	0.606	0.003	Testosterone 17beta-dehydrogenase inhibitor
0.756	0.002	Androgen agonist	0.611	0.012	Steroid N-acetylglucosaminyltransferase inhibitor
0.772	0.024	Antiseborrheic	0.604	0.005	UGT1A8 substrate
0.744	0.004	Indanol dehydrogenase inhibitor	0.610	0.018	Analeptic
0.747	0.012	Respiratory analeptic	0.603	0.012	Antipruritic, allergic
0.733	0.003	CYP2A5 substrate	0.604	0.013	UGT1A substrate
Testolactone (11)					
Pa	**Pi**	**Activity**	**Pa**	**Pi**	**Activity**
0.965	0.001	CYP19 inhibitor	0.701	0.005	CYP2A1 substrate
0.913	0.002	CYP2B5 substrate	0.697	0.002	Androgen agonist
0.900	0.006	Testosterone 17beta-dehydrogenase (NADP+) inhibitor	0.696	0.009	Antiprotozoal (Leishmania)
0.900	0.012	CYP2C12 substrate	0.699	0.015	CYP3A5 substrate
0.877	0.005	Antineoplastic	0.706	0.022	Lysase inhibitor
0.832	0.014	CYP2J substrate	0.681	0.009	Dermatologic
0.804	0.003	CYP2A4 substrate	0.651	0.010	Prostate disorders treatment
0.805	0.012	CYP2J2 substrate	0.661	0.022	Immunosuppressant
0.788	0.005	CYP3A1 substrate	0.642	0.004	Growth stimulant
0.797	0.015	CYP3A4 substrate	0.649	0.015	CYP3A4 inducer
0.783	0.004	CYP2A2 substrate	0.647	0.015	CYP3A inducer
0.792	0.015	CYP3A substrate	0.634	0.012	Ovulation inhibitor
0.765	0.009	Antiinflammatory	0.627	0.007	CYP17 inhibitor
0.745	0.005	CYP2A11 substrate	0.624	0.009	Antipruritic, allergic
0.739	0.002	Aromatase inhibitor	0.624	0.013	CYP2C11 substrate
0.741	0.008	CYP3A2 substrate	0.633	0.026	JAK2 expression inhibitor
0.758	0.027	Antiseborrheic	0.620	0.017	Acetylcholine neuromuscular blocking agent
0.733	0.004	Indanol dehydrogenase inhibitor	0.609	0.015	Antipruritic

CYP group of enzymes. Since we were interested in exploring their potential against aromatase enzyme (CYP19 group) we turned our attention toward the same. PASS results showed that

View Article Online
DOI: 10.1039/C8NJ00063H

compounds **3**, **8**, **10** and **11** have Pa values of 0.507, 0.487, 0.970 and 0.965 respectively. The support for PASS results of compound **11** comes from the fact that the same is sold under the brand name TESLAC as a well-established drug having high power of aromatase inhibition. Taking cue from the pass results we resorted to the docking studies of target compounds against CYP19 enzyme to gain insights in to their possible modes of binding with the active sites of CYP19. A thorough analysis of the binding site of enzyme aromatase using PDBsum [49] reveals that it occupies a volume of 1525.92 $^{\circ}A^3$. Also the entrance to the binding site as measured by AutoDock 4.2 was found to be 3.2 A° in diameter. Because of the small entrance cavity in aromatase bigger molecules find it difficult to reach the binding site and hence only rigid and small molecules easily diffuse inside to bind the active site as suggested by Suvannang et al. [50]. All the four compounds **3**, **8, 10 and 11** were docked to the aromatase binding site though compound **11** is a marketed drug for aromatase inhibition under the brand name TESLAC. X-ray crystal structure of human aromatase enzyme (PDB-ID 3EQM) was obtained from the Protien Data Bank web site (http://www.rrscb.org/pdb/). The preparation of target, ligand, grid and docking parameter files of all the target compounds **3**, **8, 10 and 11** was done employing AutoDock 4.2 using the Lamarkian Genetic Algorithm [51]. A grid box size of 50 x 64 x 78 A° with a grid spacing of 0.375 A° was generated using AutoGrid [52] and the grid positioned at coordinates of 83.35, 49.60, 50.60 A° which are almost reported to be the binding site residues [53]. The results obtained here provided information on the binding interactions (**Fig 5** and **6**) along with the binding free energies (ΔG_b) and inhibition constants (Ki). **Table 3** summarizes the free energies of binding and inhibition constants along with the key amino acid residues interacting with CYP19 enzyme.

View Article Online
DOI: 10.1039/C8NJ00063H

Table 3. Approximate mean binding free energies, inhibition constants and bonding interactions.

Compound	No of Rotational bonds	Best Binding energy (ΔG_b) (kcal/mol)	Inhibition Constant (Ki) (nM)	Amino acid residues of CYP19 involved in interaction with compounds
(**3**)	0	-9.85	60.09	H-bond: LEU477, SER478
(**8**)	0	-9.62	88.77	H-bonds: ARG115, LEU372, LEU477 Charge repulsion with both NH_2 protons of ARG115 Steric Bump: LEU372
(**10**)	0	-10.14	37.10	H-bonds: THR310, LEU372, SER478, TRP224 Electrostatic attraction: ASP309
(**11**)	0	-10.29	28.87	H-bonds: ARG115, PRO429, LEU372, LEU477, VAL373, PHE430 Charge repulsion with one NH_2 proton of ARG115

It is seen that Testolactum (**8**) engages in four favaourable hydrogen-bond interactions with ARG115, LEU372, PRO429, LEU477 and unfavourable interactions which include a charge repulsion with two NH_2 protons of ARG115 and a steric bump of lactum NH proton with LEU372 giving it a relatively low ΔG_b of -9.62 kcal/mol and K_i of 88.77 nM. However its close associate, Testololactum (**3**) engages only in two favourable hydrogen bond interactions with LEU477 and SER478, strong enough to give it a relatively higher ΔG_b of -9.85 kcal/mol and K_i of 60.09 nM. The slightly lower value of binding energy and inhibition constant in **8** is possibly because of unfavourable interactions which decrease the stability of the compound. On the other hand, Testololactone (**11**) was found to engage itself in five favourable interactions which include four hydrogen bond interactions with TRP224, THR310, LEU372, SER478 and an electrostatic attractive interaction with ASP309 giving a ΔG_b of -10.14 kcal/mol and K_i of 37.10 nM. However Testolactone (**11**) displayed potent inhibition as it exhibits six favourable hydrogen bond interactions with ARG115, ASP309, THR310, VAL373, LEU372, LEU477 and

View Article Online
DOI: 10.1039/C8NJ00063H

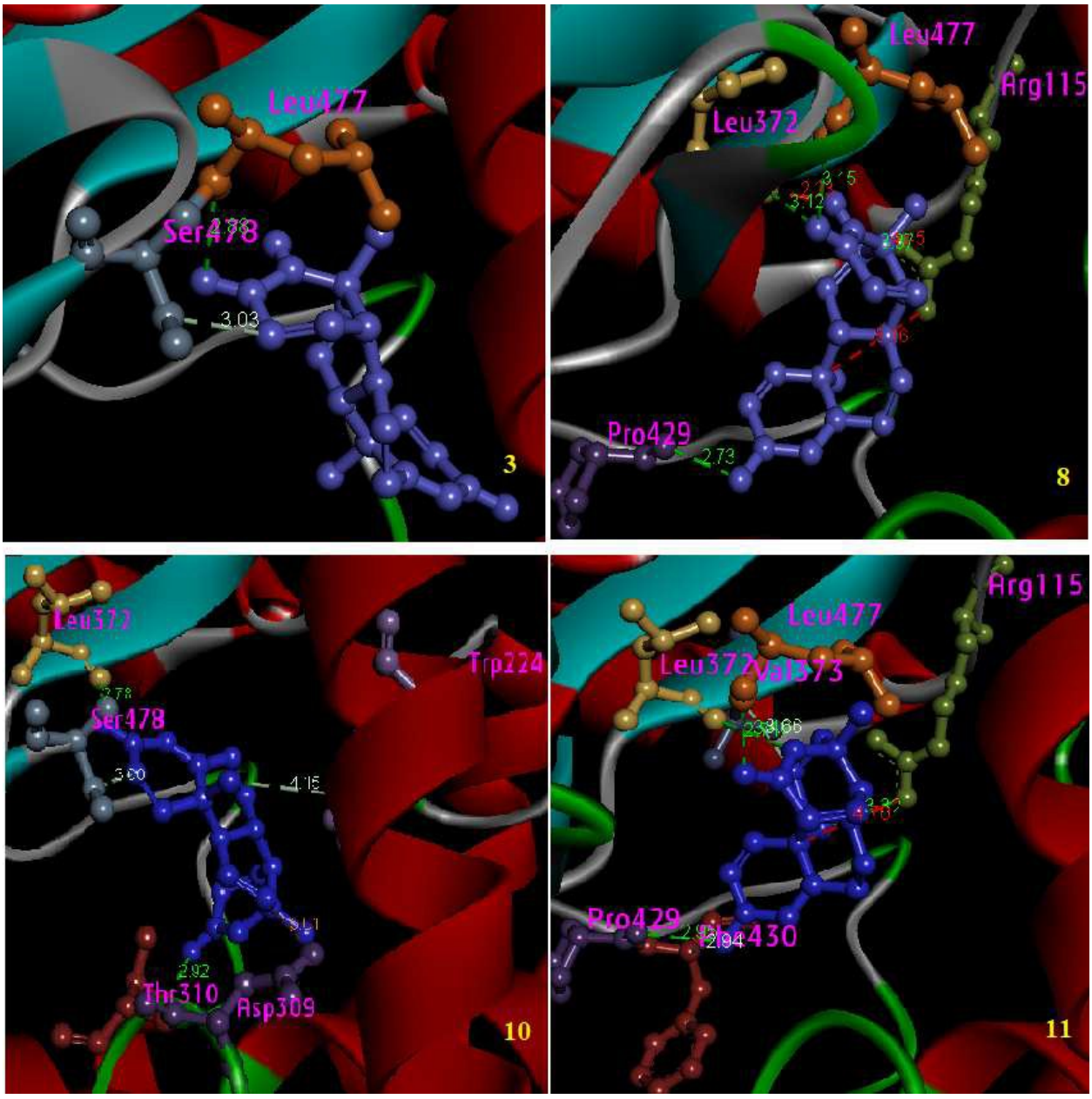

Fig 5 Best docked conformations of compounds **3**, **8**, **10** and **11.**

one unfavourable repulsive interaction with one proton of NH_2 of ARG115 sufficient enough giving it a binding free energy (ΔG_b) of -10.29 kcal and inhibition constant K_i of 28.87 nM. From the above results it is clear that compounds which possess more number of favourable hydrogen

View Article Online
DOI: 10.1039/C8NJ00063H

bond interactions with the binding site of CYP19, give more negative values of binding free energy (ΔG_b) and lowest values of inhibition constant (K_i). Also it is seen that nitrogen

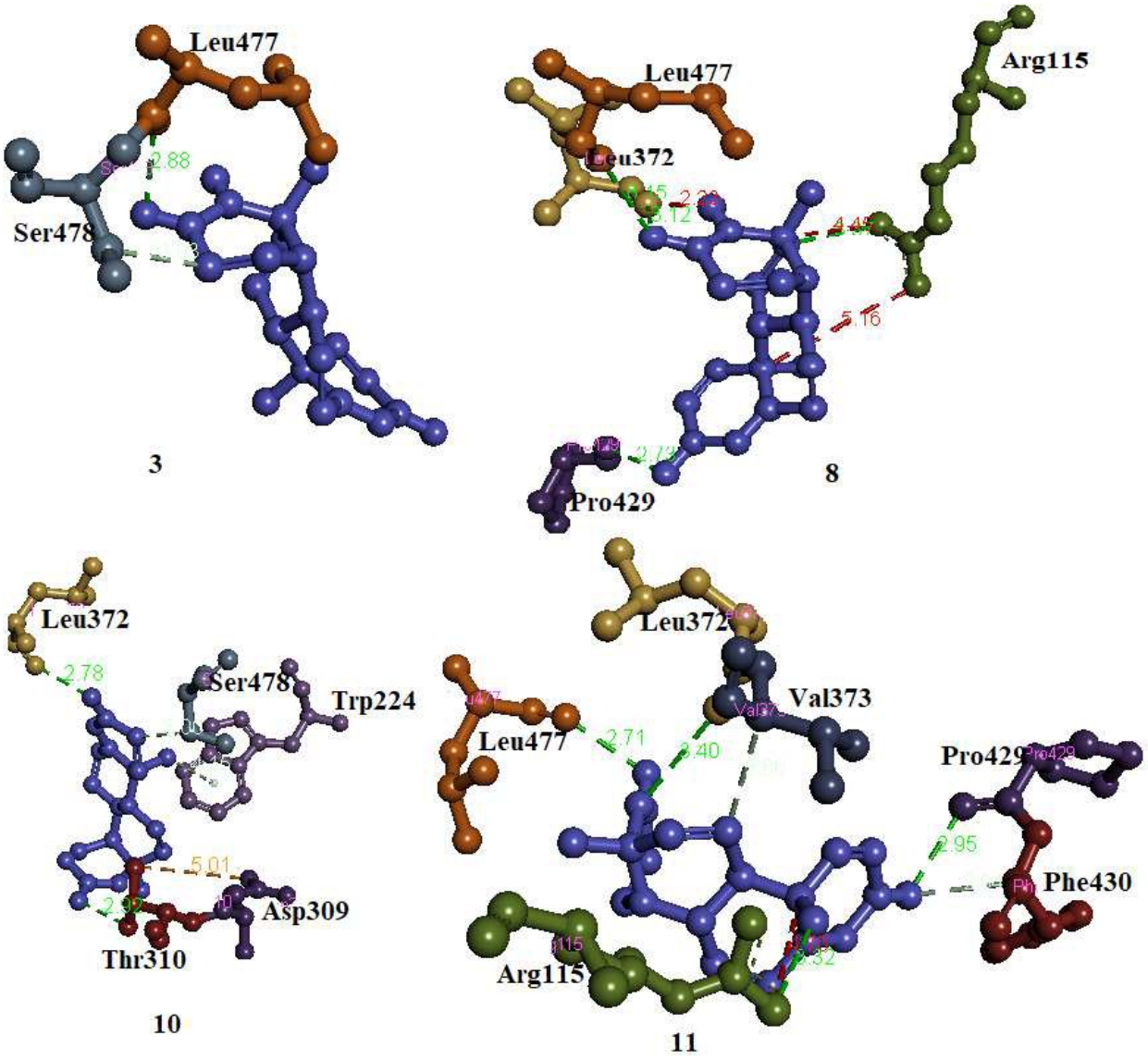

Fig 6 Amino acid residues of CYP19 enzyme binding with the compounds **3, 8, 10** and **11**.

congeners have relatively less therapeutic efficiency compared to oxygenated ones. This is possibly because in lactone containing compounds, Testololactone (**10**) and Testolactone (**11**) both O-atoms of lactone ring are involved in bonding interactions as against Testololactum (**3**)

View Article Online
DOI: 10.1039/C8NJ00063H

and Testolactum (**8**) in which only O-atom of lactam ring is involved in hydrogen bond interaction. Further Testolactum (**8**) is involved in unfavourabe interactions sufficient enough to impart it a relatively lower therapeutic efficiency as CYP19 inhibitor.

Conclusion

Testololactum (**3**) and Testolactum (**8**) were synthesized and characterized using spectral data analysis. Theoretical DFT calculations using the Becke three-parameter Lee-Yang-Parr function (B3LYP) and 6-31G (d,p) basis set were performed. MEP maps revealed that the regions with high electron density or more negative potential are concentrated over the regions spanning the carbonyl oxygen atoms of all the four compounds. FMO analysis helped to evaluate the HOMO-LUMO energy gap of all the compounds and indicates a similar nature of reactivity of the target molecules**.** PASS prediction revealed that all the four compounds are highly active against CYP19 enzyme. Molecular docking studies established that the newly synthesized steroidal lactums have the potential to be developed as aromatase inhibitors, although with relatively lower therapeutic efficiency than their corresponding oxygen containing congeners.

Experimental

General

All the solvents and reagents for the chemical synthesis were purchased from Sigma Aldrich. The chemical reactions were monitored using F_{254} silica gel TLC plates (E. Merck) using ceric ammonium sulphate as charring agent and UV chamber (366 and 254 nm) for the detection of spots. The synthesized products were purified using column chromatography on silica gel (60–120 mesh). ^{1}H NMR and ^{13}C NMR spectra (chemical shifts expressed in ppm and coupling constants in Hertz) were recorded on Bruker DPX 400 MHz spectrometer using $CDCl_3$ as the

View Article Online
DOI: 10.1039/C8NJ00063H

solvent with TMS as the internal standard. Mass spectra were carried out on LC–MS 8030 tandem mass spectrometer manufactured by Shimadzu Corporation, Kyoto, Japan. The compounds were analysed in full scan mode with nitrogen serving as interface gas. Detection was done in ESI mode having probe voltage of 180.0 V, with probe temperature of 400 ˚C. HR ESI MS was done on Agilent HRMS instrument (Model No. 6540) and all the compounds were tested for their purity using HPLC (Agilent 1260 affinity).

Synthesis

*Synthesis of compound **2**:* To a solution of compound (**1**) (2 g) in ethanol, 0.5 g of hydoxylamine hydrochloride was added in a round bottomed flask. 10 ml of deionised water and 10 ml of 10 % by wieght of aqueous NaOH solution was added and the reaction mixture heated under reflux for 2 h. The completion of reaction was monitored using TLC. The reaction mixture was evaporated under vaccuo using rotary evaporater. The residue obtained was worked up in ethyl acetate:water and washed with $NaHCO_3$ and brine. The organic layers were collected and then combined and concentrated under vaccum to yield crude residue which was purified using column chromatography to produce pure compound **2**:

*Spectral data of (10R,13S)-17-(hydroxyimino)-10,13-dimethyl-6,7,8,9,10,11,12,13,14,15,16,17-dodecahydro-1H-cyclopenta[a]phenanthren-3(2H)-one (**2**):* ^{1}H NMR (400 MHz, $CDCl_3$) δ 6.02 (s, 1H), 2.48 (s, broad, 1H, OH), 2.24 (m 5H), 2.00-1.74 (m, 3H), 1.68 (d, J= 15.7 HZ, 1H), 1.62-1.14 (m, 10H), 1.10-1.01 (m, 3H), 0.91 (s, 3H). ^{13}C NMR (101 MHz, $CDCl_3$) δ 199.21, 175.33, 171.28, 123.18, 52.63, 46.51, 45.12, 38.17, 35.89, 35.50, 34.12, 31.62, 31.09, 30.16, 29.69, 26.21, 22.12, 19.13, 14.16. ESI-MS at *m/z* = 302 for $[M+1]^+$.

*Synthesis of compound **3** and **4**:* To a solution of compound **2** (600 mg) in acetonitrile, a few drops of concentrated sulfuric acid were added and the reaction mixture heated under reflux for 3

View Article Online
DOI: 10.1039/C8NJ00063H

h in a round bottomed flask. The reaction progress was continously monitered using TLC. After completion, the reaction mixture was concentrated under vaccuo and the residue was worked up with ethyl acetate and washed with brine and $NaHCO_3$ solutions. The organic layers were collected and concentrated under vaccuo and the residue obtained was subjected to column chromatography using hexane:ethyl acetate as the eluent. A mixture of compounds (**3** and **4**) in the ratio 4 :1 was obtained.

*Spectral data of (10aR,12aS)-10a,12a-dimethyl-4,4a,4b,5,6,9,10,10a,10b,11,12,12a-dodeca hydronaphtho[2,1-f]quinoline-2,8(1H,3H)-dione (**3**):* ^{1}H NMR (400 MHz, $CDCl_3$) δ 6.03 (S, NH), 5.73 (s, 1H), 2.47-2.34 (m, 5H), 2.29-1.87 (m, 4H), 1.71-1.68 (m, 3H), 1.53-1.45 (m, 4H), 1.39-0.85 (m, 9H). ^{13}C NMR (101 MHz, $CDCl_3$) δ 199.31, 171.85, 169.87, 124.17, 54.34, 53.33, 47.32, 40.00, 38.77, 36.28, 36.19, 35.71, 34.04, 32.65, 32. 60, 22.32, 21.97, 20.50, 17.59. HR-ESI-MS at *m/z* = 302.2110 for $[M+1]^+$.

Spectral data of 10aR,12aS)-10a,12a-dimethyl-2,3,4,4a,5,6,10,10a,10b,11,12,12a-dodecahydro naphtho[2,1-f]isoquinoline-1,8(4bH,9H)-dione (**4**): ^{1}H NMR (400 MHz, $CDCl_3$) δ 6.45 (s, NH), 5.73 (s, IH), 3.50-3.09 (m, 2H), 2.54-2.23 (m, 3H), 2.18-2.09 (m, 1H), 2.09-1.85 (m, 3H), 1.82-1.41 (m, 5H), 1.39-0.92 (m, 9H), 0.90-0.68 (m, 2H). ^{13}C NMR (101 MHz, $CDCl_3$) δ 200.01, 170.57, 160.85, 119.47, 53.55, 51.22, 48.21, 44.89, 42.18, 36.85, 35.84, 35.17, 34.87, 32.85, 31.87, 22.45, 21.77, 21.18, 14.10. HR-ESI-MS at m/z = 302.2099 for $[M+1]^+$

*Synthesis of 2-phenylseleno-4-androstene-3,17-dione (**5**):* A solution of 4-androstene-3, 17-dione (**1**) (220 mg, 0.768 mmol) and phenylselenyl chloride (330 mg, 3 equivalents) in ethyl acetate (20 ml) using LDA as base was stirred at room temperature for 2 h. After the reaction was complete the solvent was removed under vaccuo and the residue was subjected to flash

View Article Online
DOI: 10.1039/C8NJ00063H

chromatography in Hex:EtOAc (75:25) to furnish 2-phenylseleno-4 androstenedione (**5**) in 75% yields.

*Spectral data of **5**:* ^{1}H NMR (400 MHz, $CDCl_3$) δ 7.30–7.24 (m, 3H), 7.11–6.87 (m,1H), 6.20 (s, 1H), 6.13 (s, 1H), 4.88 (s, 1H), 2.48 (m, 2H), 2.29 (m, 2H), 2.09 (m, 3H), 2.00 1.74 (m, 3H), 1.69 (s, 3H), 1.40–1.19 (m, 34H), 0.96 (s, 3H). ^{13}C NMR (101 MHz, $CDCl_3$) d 219.11, 185.82, 161.32, 156.32, 132.52, 129.34, 128.07, 126.85, 50.92, 49.98, 48.72, 48.41, 47.13, 43.35, 40.58, 35.83, 31.47, 30.21, 22.65, 21.73, 21.47, 13. 39. LC-ESI-MS at m/z = 441 for $[M+1]^+$ and 459 for $[M+1+H_2O]^+$.

*Synthesis of compound **6**:* To a solution of compound **5** (134 mg, 0.474 mmol) in CH_2Cl_2 was added 30% H_2O_2 solution and the reaction mixture was stirred for 4 h until complete as indicated by TLC profiling. After completion the mixture was worked up in CH_2Cl_2 and the organic layers collected. The organic layers were then combined and concentrated under vaccum to yield crude residue which was purified using column chromatography to produce pure androstenedienone (**6**) in 90% yields.

*Spectral data of 1,4-androstadien-3,17-dione **(6):*** ^{1}H NMR (400 MHz, $CDCl_3$) δ 7.00 (d, *J* = 9.8 Hz, 1H), 6.23 (s, 1H), 6.17 (d, J = 9.6 Hz, 1H), 2.54–2.39 (m, 2H), 2.37–2.27 (m, 2H), 2.15 (s, 2H), 1.97–1.81 (m, 2H), 1.48 (s, 5H), 1.30–0.88 (m, 8H). ^{13}C NMR (101 MHz, $CDCl_3$) d 221.23, 186.08, 161.29, 155.98, 127.98, 127.13, 50.99, 50.31, 48.31, 47.85, 43.65, 40.04, 35.80, 31.37, 30.53, 30.33, 22.71, 22.09, 21.79, 14.09. LC-ESI-MS at m/z = 285 for $[M+1]^+$ and 326 for $[M+1+ACN]^+$.

Synthesis of compound 7: To a solution of compound (**6**) (100 mg) in ethanol was added 25 g of Hydoxylaminehydrochloride in a round bottomed flask. 2 ml of deionised water and 2 ml of 10 % by wieght of aqueous NaOH solution was added and the reaction mixture heated under reflux

View Article Online
DOI: 10.1039/C8NJ00063H

for 1.5 h. The completion of reaction was monitored using TLC. The reaction mixture was evaporated under vaccuo using rotary evaporater. The residue obtained was worked up in ethyl acetate:water and washed with $NaHCO_3$ and brine. The organic layers were collected and then combined and concentrated under vaccum to yield crude residue which was purified using column chromatography to produce pure compound **7**:

Spectral data of (10R,13S)-17-(hydroxyimino)-10,13-dimethyl-6,7,8,9,10,11,12,13,14,15,16,17-dodecahydro-3H-cyclopenta[a]phenanthren-3-one (7): ^{1}H NMR (400 MHz, $CDCl_3$) δ 7.10 (d, J = 9.8 Hz, 1H), 6.21 (s, 1H), 6.10 (d, J = 9.6 Hz, 1H), 2.58 (br s, OH), 2.51-2.36 (m, 2H), 2.31 - 2.25 (m, 2H), 2.12 (s, 2H), 1.97-1.48 (m, 6H), 1.36-0.90 (m, 9H). ^{13}C NMR (101 MHz, $CDCl_3$) δ 185.32, 174.18, 167.39, 155.31, 127.21, 127.16, 50.86, 48.76, 48.10, 44.33, 42.70, 40.18, 31.67, 30.02, 26.14, 23.63, 22.97, 20.51, 14.06. LC-ESI-MS at *m/z* = 300 for $[M+1]^+$.

*Synthesis of compound **8** and **9**:* A solution of compound **7 (**80 mg**)** in acetonitrile, was added few drops of concentrated sulfuric acid and the reaction mixture heated under reflux for 3 h in a round bottomed flask. The reaction progress was continously monitered using TLC. After completion, the reaction mixture was concentrated under vaccuo and the residue was worked up with ethyl acetate and washed with brine and $NaHCO_3$ solutions. The organic layers were collected and concentrated under vaccuo and the residue obtained was subjected to column chromatography using hexane:ethyl acetate as the eluent. A mixture of compounds (**8** and **9**) in the ratio 4 :1 was obtained.

*Spectral data of Testolactum (**8**):* ^{1}H NMR (400 MHz, $CDCl_3$) δ 7.00 (d, J = 8 Hz, 1H), 6.24-6.21 (m, 2H), 6.06 (s, 1H), 2.51-2.28 (m, 2H), 2.25 -1.75 (m, 6H), 1.72-1.52 (m, 2H), 1.48-1.26 (m, 8H). ^{13}C NMR (101 MHz, $CDCl_3$) δ 186.24, 171.93, 167.96, 154.82, 128.23, 124.18, 54.40,

View Article Online
DOI: 10.1039/C8NJ00063H

51.77, 47.14, 43.35, 39.80, 36.16, 32.57, 30.62, 22.94, 22.74, 22.32, 20.45, 18.93. HR-ESI-MS at *m/z* = 300.1955 for $[M+1]^+$.

Density Functional Theory study

All the computations are carried out using GAUSSIAN 09 software [54]. The DFT modeling method, using the hybrid B3LYP [55] functional was used to calculate theoretical parameters for target compounds with the basis set combination 6-31 G (d, p) [56]. Geometry optimization was carried out until global minima were achieved.

Acknowledgement

SHL thanks DST-SERB India for financial grant supporting this work in the form of a project under the scheme National Postdoctoral Fellowship (NPDF, File No. PDF/2016/001690/CS).

Conflict of interest

The authors declare no conflict of interest.

Supplementary Information

^{1}H, ^{13}C NMR and Mass spectra are available in the form of Supplementary information with this article and can be availed free of cost from the online version.

References

1 E.T.H. Fontham, M.J. Thun, E. Ward, A.J. Balch, J.O.L. Delancey, J. M. Samet. *CA Cancer J. Clin*. 2009, **59**, 343-351.

2 Cancer facts & figures 2008. American Cancer Society.

3 R. W. Brueggemeier, J. C. Hackett, E. S. Az-Cruz, *Endocr. Rev.* 2005, **26**, 331.

4 J. Russo, M. H. Lareef, G. Balogh, S. Guo, I. H. Russo, *J. Steroid. Biochem. Mol. Biol*. 2003, **87**, 1-25.

5 B. Meunier, S. P. de Visser, S. Shaik, *Chem Rev.* 2004, **104**, 3947.

View Article Online
DOI: 10.1039/C8NJ00063H

6 D. Cunningham, T. J. Powles, M. Dowset, G. Hutchison, A. M. H. Brodie, H. T. Ford, J. C. Gazet, R.C. Coombes. *Cancer Chemother. Pharm*. 1987, **20**, 253-255.

7 P. Lombardi. *Biochim Biophys Acta*, 2002, **1587**, 326–37.

8 X. Wang, S. Chen, *Cancer Research*, 2006, **66**, 10281-10286.

9 R. L. Prairie, P. Talalay, *Biochemistry*, 1963, **2**, 203–8.

10 H. M. Liu, H. Li, L. Shan, J. Wu. *Steroids* 2006, **71**, 931–4.

11 T. Kolek, A. Szpineter, A. Swizdor. *Steroids* 2009, **74**, 859–62.

12 A. C. Hunter, N. E. Carragher. *J Steroids Biochem Mol Biol* 2003, **87**, 301–8.

13 B. Yang, Y. Wang, X. Chen, J. Feng, W. Qiaqing, Z. Dumming. *Tetrahedron* 2014, **70**, 41–6.

14 H. Zhang, R. Jie, Y. Wang, C. Sheng, W. Qiaqing, A. Diao et al. *Tetrahedron* 2013, 69, 184–9.

15 S. H. Lone, K. A. Bhat. *Steroids* 2015, **96**, 164–168.

16 L. W. Lawrence Woo, C Bubert, O. B. Sutcliffe, A. Smith, S. K. Chander, M. F. Mahon, A. Purohit, M. J. Reed, B. V. L. Potter. *J. Med. Chem.* 2007**, 50***,* 3540-3560.

17 Y. Dai, Q. Wang, X. Zhang, S. Jia, H. Zheng, D. Feng, P. Yu. *European Journal of Medicinal Chemistry* 2010, **45**, 5612-5620.

18 P.P. Roy, K. Roy. *J. Mol Model*. 2010, **16**, 1597-1616.

19 A. H. Abadi, S. M. Abou-Seri, Q. Hu, M. Negrid R. W. Hartmann. *Med. Chem. Commun*, 2012, **3**, 663-666.

20 V. Prachyawarakorn, S. Sangpetsiripan, P. Surawatanawong, C. Mahidol, S. Ruchirawat, P. Kittakoop. *Med. Chem. Commun*. 2013, **4**, 1590-1596.

View Article Online
DOI: 10.1039/C8NJ00063H

21 R. Pingaew, V. Prachayasittikul, P. Mandi, C, Nantasenamat, S. Prachayasittikul, S. Ruchirawat, V. Prachayasittikul. 2015, ***23,*** 3472-3480.

22 S.H. Lone, K.A. Bhat, S. Rehman, R. Majeed, A. Hamid, M.A. Khuroo, *Bioorg. Med. Chem. Lett.* 2013, **3**, 4931–4934.

23 S. Naseer, S.H. Lone, J. A. Lone, M.A. Khuroo, K.A. Bhat. *Journal of Chromatography B*. 2015, 989, 62–70.

24 S.H. Lone, K.A. Bhat. R. Majeed, A. Hamid, M.A. Khuroo, *Bioorg. Med. Chem. Lett.* 2014, **24**, 1047–1051.

25 S.H. Lone, K.A. Bhat, *Tetrahedron Lett*. 2015, **56**, 1908–1910.

26 I. Ayoob, S.H. Lone, M. Rahman, O.A. Zargar, R. Bashir, S. Rehman, M. A. Khuroo, K. A. Bhat, ChemistrySelect, 2017, **2**, 10153-10156.

27 S. Rehman, K. A. Bhat, S. H. Lone, F. A. Malik, Arab. J. Chem. 2015, https://doi.org/10.1016/j.arabjc.2015.10.009

28 S. Rehman, B. Rah, S.H. Lone, R. Rasool, S. Farooq, D. Nayak, N.A. Chikan, S. Chakraborty, A. Behl, D.M. Mondhe, A. Goswami, K.A. Bhat, *J. Med. Chem*. 2015, **58**, 3432-3444.

29 S.H. Lone, K.A. Bhat, F.A. Malik, M.A. Khuroo, *Planta Med Int Open*. 2016, **3**, 51–54.

30 S.H. Lone, S. Rehman, K.A. Bhat, *Drug Res.* (Stuttgart, Ger.) 2017, 67, 111–118.

31 B. A. Dar, S.H. Lone, W.A. Shah, K.A. Bhat. *Drug Res.* (Stuttgart, Ger.) 2016, **66**, 427-431.

32 I. Ayoob, Y.M. Hazari, S.H. Lone, S. Rehman, M.A. Khuroo, K.M. Fazili, K.A. Bhat, *ChemistrySelect.* 2017, **2**, 2965–2968.

View Article Online
DOI: 10.1039/C8NJ00063H

33 S. H. Lone, K. A. Bhat, S. Naseer, R. A. Rather, M. A. Khuroo, S. A. Tasaduq, *J. Chromatogr. B* 2013, **940**, 135–141.

34 K. Abhishek, K.S. Ambrish, G. Shashi, M. Neeraj, M. Avijit, B. Goutam, *J. Mol. Struct.* 2015, **1096**, 94–101.

35 M. N. Arshad, A. Bibi, T. Mahmood, A.M. Asiri, K. Ayub, *Molecules* 2015, **20,** 5851–5874.

36 H. Zhou, J. Skolnick, *Mol. Pharm*. 2012, **9***,* 1775–1784.

37 E. Scrocco, J. Tomasi*, Adv. Quantum Chem*. 1979, **11***,* 115-193.

38 N. Okulik, A. H. Jubert, *J. Mol. Des*. 2005, **4**, 17-30.

39 K. Fukui, T. Yonezawa, H. J. Shingu, *J. Chem. Phys*. 1952, **20**, 722–725.

40 R. A. Costa, P. O. Pitt, M. L. B. Pinheiro, K. M. T. Oliveira, K. S. Salome, A. Barison , E. V. Costa. *Spectrochimica Acta Part A: Molecular and Biomolecular Spectroscopy* 2017, **174**, 94–104.

41 R. A. Costa, K. M.T. Oliveira, E. V. Costa, M. L. B. Pinheiro. *J Molecular Structure* 2017, **1145**, 254-267.

42 N. Özdemir, S. Dayan, O. Dayan, M. Dinçer, N. Kalaycıoglu, *J. Mol. Phys*. 2013, **11 (6)** 707–723.

43 R. Parr, Functional Theory of Atoms and Molecules, Oxford University Press, New York, 1989.

44 R. Parr, L. Szentpaly, S. Liu, *J. Am. Chem. Soc* 1999, **121**, 1922–1924.

45 J. F. Janak, *Phys. Rev. B* 1978, **18**, 7165.

46 J. P. Perdew, R.G. Parr, M. Levy, J. L. Balduz Jr., *Phys. Rev. Lett*. 1982, **49**, 1691-1694.

View Article Online
DOI: 10.1039/C8NJ00063H

47 A. Lagunin, A. Stepanchikova, D. Filimonov, V.Poroikov, *Bioinformatics* 2000, **16**, 747-748.

48 R. Pramely, T.L.S. Raj, *J. Biochem. Tech* 2012, **3**, 375-379.

49 R. A. Laskowski, E. G. Hutchinson, A, D. Michie, A. C. Wallace, M. L. Jones, J. M. Thornton. *Trends. Biochem. Sci*. 1997, **22**, 488-490.

50 N. Suvannang, C. Nantasenamat, C. Isarankura-Na-Ayudhya, V. Prachayasittikul, Molecules, 2016, ***16,*** 3597-3617.

51 F. J. Solis, R. J. B. Wets. *Math Oper. Res*. 1981, 6, 19-30.

52 G. M. Morris, D. S. Goodsell, R. S. Halliday, R. Huey, W. E. Hart, R. K. Belew, A .J. Olson. *J. Comput. Chem.,* 1998, **19**, 1639–1662.

53 D. Ghosh, J. Griswold, M. Erman, W. Pangborn, *Nature,* 2009, **457,** 219-223.

54 M. J. Frisch, G. W. Trucks, H. B. Schlegel, G. E. Scuseria, M. A. Robb, J. R. Cheeseman, G. Scalmani, V. Barone, B. Mennucci, G. A. Petersson, H. Nakatsuji, M. Caricato, X. Li, H. P. Hratchian, A. F. Izmaylov, J. Bloino, G. Zheng, J. L. Sonnenberg, M. Hada, M. Ehara, K. Toyota, R. Fukuda, J. Hasegawa, M. Ishida, T. Nakajima, Y. Honda, O. Kitao, H. Nakai, T. Vreven, J. A. Montgomery, Jr., J. E. Peralta, F. Ogliaro, M. Bearpark, J. J. Heyd, E. Brothers, K. N. Kudin, V. N. Staroverov, T. Keith, R. Kobayashi, J. Normand, K. Raghavachari, A. Rendell, J. C. Burant, S. S. Iyengar, J. Tomasi, M. Cossi, N. Rega, J. M. Millam, M. Klene, J. E. Knox, J. B. Cross, V. Bakken, C. Adamo, J. Jaramillo, R. Gomperts, R. E. Stratmann, O. Yazyev, A. J. Austin, R. Cammi, C. Pomelli, J. W. Ochterski, R. L. Martin, K. Morokuma, V. G. Zakrzewski, G. A. Voth, P. Salvador, J. J. Dannenberg, S. Dapprich, A. D. Daniels, O. Farkas, J. B.

View Article Online
DOI: 10.1039/C8NJ00063H

Foresman, J. V. Ortiz, J. Cioslowski, D. J. Fox, Gaussian 09, B. 01, Gaussian, Inc., Wallingford CT, 2010.

55 (a) A.D. Becke, *Journal of Chemical Physics*, 1993, **98**, 1372-1378 (b) P. J. Stephens, F. J. Devlin, C. F. Chabalowski, M. J. Frisch, *Journal of Physical Chemistry* B, 1994, **98**, 11623.

56 (a) A.D. McLean, G.S. Chandler, *Journal of Chemical Physics* 1980, **72**, 5639 (b) K. Raghavachari, J. S. Binkley, R. Seeger and J. A. Pople, *Journal of Chemical Physics*, 1980, **72**, 650. (c) J. P. Blaudeau, M. P. McGrath, L. A. Curtiss, L. Radom, *Journal of Chemical Physics*, 1997, **107**, 5016 (d) A. J. H. Wachters, *Journal of Chemical Physics*, 1970, **52**, 1033 (e) P. J. Hay, *Journal of Chemical Physics*, 1977, **66**, 4377. (f) K. Raghavachari, G. W. Trucks, *Journal of Chemical Physics*, 1989, **91**, 1062 (g) R. C. Binning Jr., L. A. Curtiss, *Journal of Computational Chemistry*, 1990, **11**, 1206 (h) M. P. McGrath, L. Radom, *Journal of Chemical Physics*, 1991, **94**, 511 (i) L. A. Curtiss, M. P. McGrath, J. P. Blaudeau, N. E. Davis, R. C. Binning Jr. and L. Radom, *Journal of Chemical Physics*, 1995, **103**, 6104.

View Article Online
DOI: 10.1039/C8NJ00063H

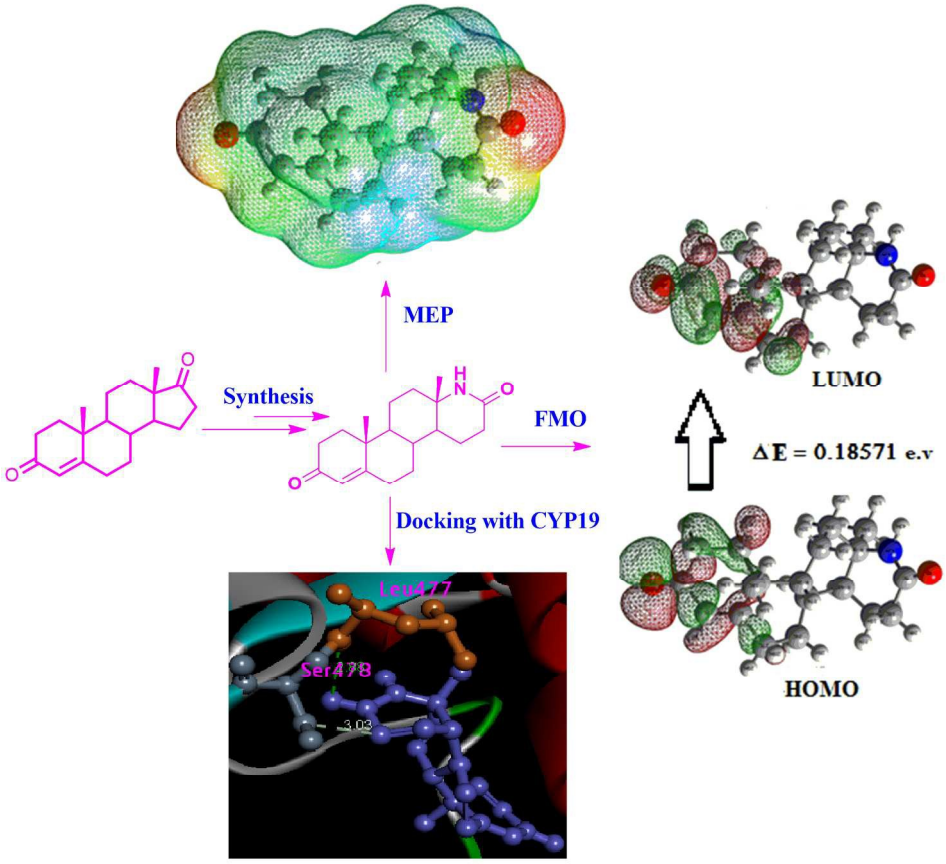

Combined DFT and Molecular Docking studies of synthesized steroidal lactums reveal their potential as Aromatase Inhibitors.

186x182mm (300 x 300 DPI)